Evaluation of a Novel Passive Safety Concept for Motorcycles with Combined Multi-Body and Finite Element Simulations.

Steffen Maier, Laurent Doléac, Holger Hertneck, Sebastian Stahlschmidt, Jörg Fehr

Abstract The objective of this research is to investigate a novel passive safety concept for motorcycles that, in the event of an accident, guides and controls the trajectory of the rider and thereby enables better protection with passive safety systems. The concept, a newly designed motorcycle body in combination with thigh belts, multiple airbags, impact protectors and side protection structure, restrains the rider to the motorcycle and the motorcycle and its safety equipment form a protective cover around the rider.

In this study, the motorcycle and safety concept are entirely modelled in a combined multi-body and finite element approach in the MADYMO software environment. The motorcycle and rider surrogate, a dummy, were simulated in seven accident scenarios for motorcycles colliding with passenger cars, according to ISO13232. The crashworthiness, i.e. the kinematics, the force interactions and the biomechanical loads on the main body parts of the rider, were analysed with respect to the biomechanical limits.

Restraining the rider with belts and decelerating the resulting upper body motion relative to the motorcycle with multiple surrounding airbags led to a guided and controlled dummy trajectory for the primary accident phase, showing promising performance of the innovative solution for rider protection for multiple accident scenarios.

Keywords Motorcycle safety, motorcycle to car collisions, multi-body simulations, passive safety, vulnerable road users.

I. INTRODUCTION

Motorcycles are enjoying growing popularity as a compact means of transport in congested cities and as a leisure or lifestyle object with a recently general positive trend in registration numbers in Europe from 2013 to 2018 [1]. Especially in combination with an electric powertrain, motorcycles have a high potential as agile, space-saving and clean mobility solutions in cities. Driven by the highly topical debates on driving bans due to excessive nitrogen oxide and fine dust pollution, the increased switch to motorcycles can make a substantial contribution. The better carbon footprint and lower fuel and energy consumption offer a cost-effective improvement in the traffic situation and pollutant emissions.

However, motorcycle accidents, though not necessarily more frequent than accidents involving other road users, are much more likely to be severe or fatal. The probability of a fatal motorcycle accident is many times higher than that of a passenger car, based on registration figures and considering the lower mileage of motorcycles. Globally, approximately 375,000 people die in accidents of two and three-wheelers annually [2]. More specifically i.e. Germany recorded 31,204 injuries in motorcycle accidents with 619 fatalities, accounting for 18.9 % of all road traffic deaths [3]. The high mortality rate in motorcycle accidents is due to the low level of passive protection of the occupants of motorcycles. This is a considerable shortcoming that can deter potential users of motorcycles.

The proposed novel safety concept for motorcycles consists of a newly designed motorcycle body and a combination of seat belts, several airbags, impact protectors and side protection structure. In the event of an accident, the rider is fixed to the motorcycle and the motorcycle body and its safety equipment form a protective cover around the rider. The goal is to supersede a motorcycle rider's safety clothing and helmet entirely in the future and to significantly increase the suitability of motorcycles as commuter vehicles and/or shared mobility solutions. By increasing the passive safety of motorcycles, more people can be motivated to switch to

S. Maier (steffen.maier@itm.uni-stuttgart.de, +49 711 685-66956) is a Research Associate and Doctoral student at the Institute of Engineering and Computational Mechanics (ITM) at the University of Stuttgart, Germany. L. Doléac is the founder of Doléac Models, Ostfildern, Germany. H. Hertneck is Director of Sales and Development at SASTEC GmbH, Markgroeningen, Germany. S. Stahlschmidt is Head of the Competence Field Dummy Models at DYNAmore GmbH, Stuttgart, Germany. J. Fehr is Professor at the Institute of Engineering and Computational Mechanics (ITM) at the University of Stuttgart, Germany.

motorcycles, so that the advantages mentioned above become more pronounced. As a result of this, the concept significantly improves passive safety without compromising a motorcycle's specific advantages as a compact means of transport and without losing its unique driving behaviour.

As very recently summarised by [4], previous and current efforts to improve the passive safety of motorcycles include personal protective equipment (safety clothing, helmets, neck braces, wearable airbag devices), airbags mounted to the motorcycle, belts and enveloping structures. Although still a rare standard equipment, motorcycle-mounted airbags were summarized as effective devices to reduce impact velocities especially in frontal crashes but have limited effect in oblique collisions with a moving opponent. Reference [4] proposed a wearable belted safety jacket that was able to reduce head and neck loading for a collision between motorcycle and a moving car for ISO 13232 configuration 413 – 6.7/13.4 (see Fig. 5) because dummy head to car impact was prevented. Murri [5] investigated a harness system consisting of shoulder, pelvis and crotch belts for motorcycle riders to avoid the rider's head to crash opponent contact, shown for a similar collision configuration at varying speeds. To prevent pitching of the motorcycle around its transverse axis and excessive upward motion of the rear, a crash box was used in the front fairing. So far the BMW C1 scooter [6] remains the only two-wheeler ever in series production that features belt restraints for the motorcyclist. In combination with a safety cell it offers a high level of passive protection and is therefore licensed for non-helmet use in most countries. The novelty of the concept presented here is the first attempt to use a whole combination of safety components, interacting with each other, to protect motorcyclists. This approach is comparable to passive safety systems for car occupants, where a combination of several safety components also has proven to be effective.

This work aims to investigate the effectiveness of the novel safety concept by evaluating its performance on a variety of recommended accident scenarios, representing frequent real-world motorcycle accidents. This was done via simulations, predicting the accident kinematics of the motorcycle and rider, as well as resulting biomechanical body loads. Results of the simulations will be shown for the primary accident phase, the immediate period after the first impact, and biomechanical limits and injury probabilities will be discussed.

II. METHODS

Experimental investigations with prototypes are costly and time-consuming. Furthermore, the protective effect of the system for the occupant depends on a multitude of components and parameters interacting with each other. For systematic design and optimisation, a simulative approach has therefore been used. In this early and first stage of a multi-phase research project, the motorcycle and safety concept have been modelled in a combined multi-body (MB) and finite element (FE) approach in the MADYMO software environment (version MADYMO 7.8). The motorcycle and rider, substituted by an anthropomorphic test device, were simulated in seven representative accident scenarios for motorcycles colliding with passenger cars to predict the performance of the proposed safety concept. The combined MB and FE approach in combination with advanced and validated dummy models in MADYMO for multiple accident scenario simulations represent a numerical efficient way to continuously tune and improve the safety system, i.e., adapting the properties, shapes and locations of the safety components.

Motorcycle Multi-body Model and Motorcycle Rider Surrogate

To replicate its crash dynamics, significant parts of the motorcycle were modelled with a rigid body model consisting of three bodies shown in the schematic in Fig. 1. These are the body of the motorcycle, the front and rear wheel, reflected by their geometry, mass (m), and moments of inertia (I). The main features of the model are the couplings of (i) rotating wheels, (ii) front and rear suspension, (iii) front fork steering, and (iv) front fork impact deformation with kinematic joints, constraining the relative motion of the parts. The coupling of front and rear suspension involves nonlinear spring restraints $c_{\mathrm{F}}(s)$, $c_{\mathrm{R}}(\theta)$, dependent on front suspension deflection s and rear suspension deflection angle θ, and constant dampening restraints d_{F}, d_{R}. A moment restraint $M_{\mathrm{def}}(\varphi)$ implements the deformation of the telescopic front fork with fork impact deflection angle φ using MADYMO load characteristic, as shown in Fig. 2. The front fork impact deflection has been approximated with a linear elastic response up to the elastic limit φ_{e}. For higher impact deflection angles, the implemented loading characteristics represent at first failure with plastic deformation of the front fork and then collision of the front wheel with the motorcycle body according to $M_{\mathrm{def,\ loading}}(\varphi)$ with unloading characteristics parallel to the hysteresis slope and along $M_{\mathrm{def,\ unloading}}(\varphi)$.

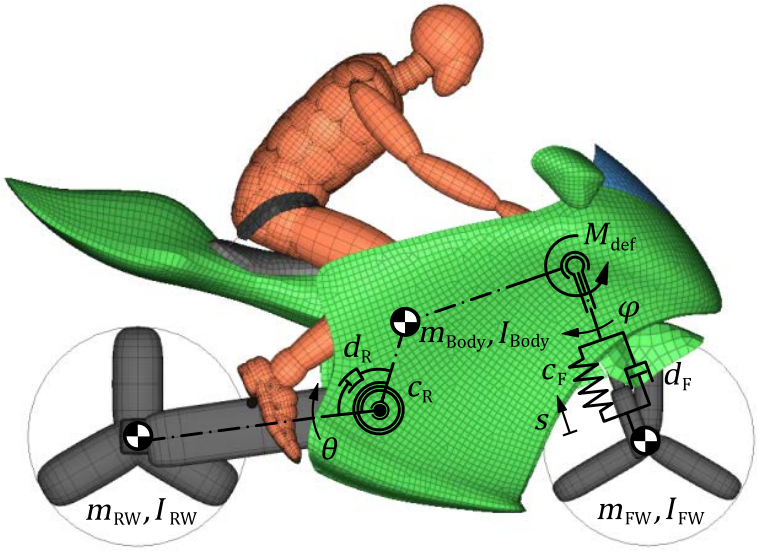

Fig. 1. Motorcycle MB model, consisting of body front (FW) and rear wheels (RW) with non-helmeted Hybrid III 50th percentile adult male dummy in sitting configuration.

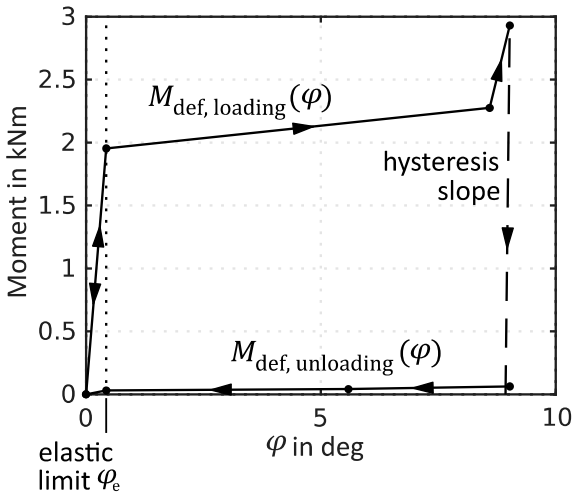

Fig. 2. Loading and unloading characteristics $M_{\text{def}}(\varphi)$ of the telescopic front fork impact deformation.

The shown front fork restraint characteristics, as well as the implemented contact interaction characteristics and parameters between the components of the motorcycle and the accident opponent, a passenger car, have been based on fitted simulation models of full-scale crash tests of conventional motorcycles and Hybrid III 50th percentile dummys in sitting configuration colliding with cars from Dekra [7]. Crash tests SH 01.01 and SH 99.27 were fitted using the Dekra documentation and sensor data. Comparisons of motion sequence and acceleration sensor data of the simulations and experiments are given in Appendix A. For test SH 01.01, a motorcycle impacting at 48.5 km/h at a right angle into the side of the stationary car, shown in Fig. A1 and Fig. A2, the motorcycle and car trajectories and accelerations conform well. Merely initial immersion of the suspension of the impact side and as a result similar helmet impact location at the car could not be achieved with the MB approach. In test SH 99.27, shown in Fig. A3 and Fig. A4, the motorcycle impacted with 47.8 km/h at a right angle into the side of the car travelling at 23.9 km/h. The comparison shows similar motions of motorcycle and car as well as conforming peak accelerations. The difference of motorcycle motion of the two experiments and respective simulations also illustrates that pitching of the motorcycle around its transverse axis is dependent whether the motorcycle has sufficient deformation structure in front of the stiff fork head and therefore a high contact point. Also, the Yamaha GTS 1000 in test SH 99.27 has a forkless front suspension, a single-sided swing arm, which appears to be weak in case of a frontal collision. Compared to the Yamaha FZS 600 Fazer from test SH 01.01 the front fork of the proposed motorcycle was defined to be sufficiently stiffer. The loading and unloading characteristics of the front fork deformation shown in Fig. 2 are scaled by factors of 3 in y-direction and 0.75 in x-direction. Also, compared to the Yamaha GTS 1000 from test SH 99.27, the proposed motorcycle was simulated using stiffer contact characteristics between motorcycle body and car. Contact loading and unloading force vs. deformation curves of the motorcycle body to car contact were scaled by a factor of 2 for the forces.

Despite the recommendation of Norm ISO 13232-3:2005 [8], which specifies methods and procedures for the assessment of motorcycle protection devices, to use the motorcyclist anthropometric test device (MATD) with sit/stand pelvis we used a Hybrid III 50$^{\text{th}}$ percentile male ellipsoid surrogate model. The modifications of the MATD include (i) a modified neck and head compatible with motorcycle helmets and for motorcycle-specific head positioning, (ii) sit/stand pelvis, (iii) dummy hands for wrapping around handlebars and (iv) frangible components in the abdomen, upper and lower legs, and knees. The reasons for using the Hybrid III instead of the specially modified MATD dummy include: (i) the MATD has significant clefts at the hip attachment points not suited to fasten thigh belts, (ii) a helmet is not worn, helmet compatibility is no requirement, (iii) the Hybrid III also used in in the simulation models of full-scale crash tests of Dekra, and (iv) the MATD dummy is not available as a FE model in LS-DYNA, which will be used in the next step of the research.

Initially, multiple bodies of the dummy's extremities were fixed relative to the motorcycle to freeze the position and posture of the dummy while allowing for settling initial contacts and suspension coupling. At impact, after about 100 ms, these constraints were automatically released.

Passive Safety Components

The passive safety components of the concept shown in Fig. 3, consisting of two thigh belts and in total five airbags surrounding the rider, have been modelled using the FE capabilities of MADYMO. The proposed leg impact protection has not yet been included. This will be modelled in a more detailed approach in the LS-DYNA software environment. For improved simulation performance, only one half of the airbag protection has been considered, omitting the mirrored airbag components. To model the inflation process, the initial metric method with a scaled initial and an undeformed designed 2D FE membrane mesh of the airbag fabric was used. For expansion uniform pressure of ideal gases in the airbag chamber, dependent on state variables pressure and temperature, has been assumed. Therefore, the design variables for deployment, apart from the implemented material model of the fabric, include the external and internal geometry of the airbag, a scalable mass flow rate with constant inflow temperature and a scale factor for the exhaust hole area.

The front airbag used is a 38 litre 3D airbag in a wedge shape with no internal structure and two exhaust outlets, regulating the airbag pressure and consequentially the rider's deceleration when impacting. The airbag was placed centred in front of the rider and attached on its underside to the motorcycle. The front airbag is intended to ultimately be covered by a removable lid. The attachment of the windshield has been designed to fail under contact pressure of the expanding front airbag to allow more forward displacement of the rider in case of airbag deployment. Here, this was approximated as a restrained revolute joint between windshield and motorcycle body, activated after an initial break free moment.

The two mirror airbags were designed to expand from within the two rear-view mirrors. To accommodate space for the rider's lower arms and hands the airbags used are smaller, 22 litres round 2D airbags with no internal structure and one exhaust openin each. The airbag lids, initially covering the airbags, also act as reaction structures for the inflated airbags supporting the back of them. The lids were connected to the rear-view mirrors by a hinge on their upper edge which pushed away and rotated into place by the airbag deployment force.

The two side airbags placed on each side of the rider are 75 litre 2D airbags attached to the motorcycle through their lower edges. Internally nine tethers each connect the inward and outward facing fabrics to limit the lateral deployment and achieve a flat shape with large faces. The side airbags were designed to have no exhaust openings to keep them inflated at around 0.1 bar for a potentially long secondary accident phase.

The belts, placed around the thighs of the rider, were modelled using 2D finite membrane elements for the sections in contact with the dummy. One dimensional MB belt segments connect the belts to the motorcycle body attachment points. On each of the two outer belt attachments, a belt pretensioner combined with a belt load limiter was implemented. As shown in Fig. 4, the desired belt pay-in for pretensioning has been defined as a function of time. In an accident, the belt is continuously drawn in until an implemented force limit is reached. For further belt pay-out during the accident, this force limit is further applied to provide a constant force level and thus reducing peak forces and peak deceleration of the dummy. Apart from initial belt routing the design variables include the belt geometry, the positions of the attachment points, the belt pay-in function and belt load limit.

Following findings of sensor concepts of accident detection for motorcycles in [9], i.e. based on front fork deceleration, and specifications of the Honda Gold Wing sensor system in [11], the interval between the motorcycle-car contact and the time to fire time for airbags and pretensioner was fixed to 12 ms. The achieved deployment time to full volume for the airbags is approximately equal at 30 ms.

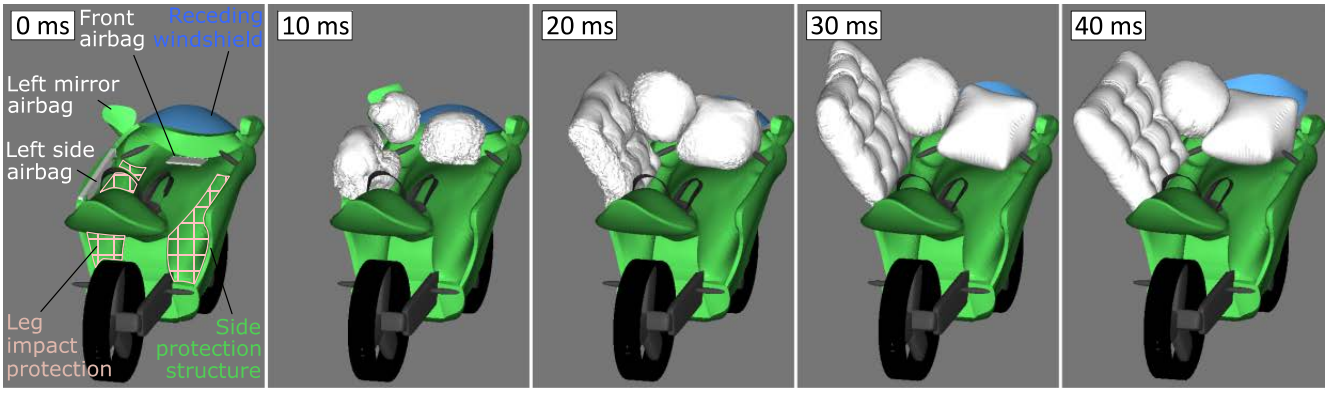

Fig. 3. Overview of components of safety concept and inflation process of the front airbag, the left mirror airbag and the left side airbag, representing the left half of the concept's airbag protection.

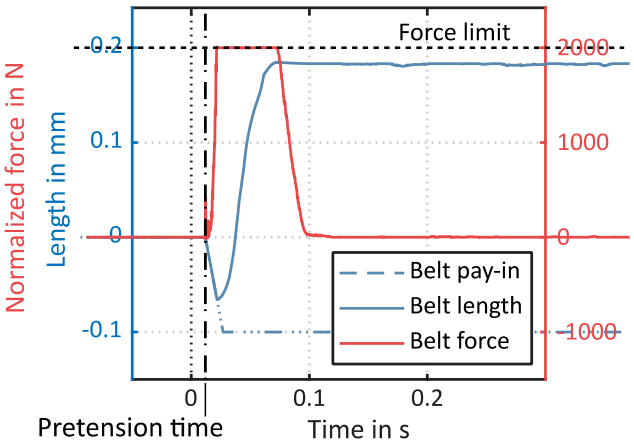

Fig. 4. Desired belt pay-in, actual belt length and resultant belt force for the belt pretensioners and load limiters.

Impact Configurations

The motorcycle and rider were simulated in seven representative accident scenarios for motorcycles colliding with passenger cars, according to ISO 13232-2:2005 [8]. The impact configurations, shown in Fig. 5, represent very frequent accidents, recommended based on 501 real motorcycle to car accidents in Hannover (Germany) and Los Angeles (USA). Each impact configuration with nomenclature XXX – YY/ZZ is identified by a three-digit code XXX, indicating relative geometric positions of the motorcycle and the opposing vehicle at impact, followed by the speeds at impact in meters per second of the opponent vehicle YY and motorcycle ZZ.

Concordant with the ISO 13232-6:2005 [8] the opposing vehicle was represented by a 1987 Ford Scorpio, a four-door saloon with a mass of 1,410 kg, overall height of 141 cm and with vehicle parameters according to [10].

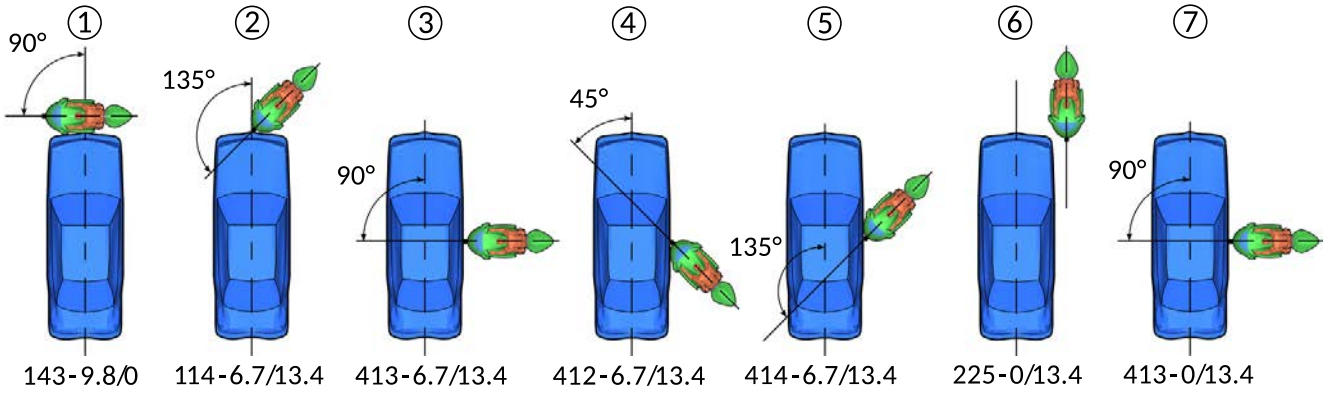

Fig. 5. Impact configurations ① to ⑦ of motorcycle and occupant vehicle according to ISO 13232:2005.

III. RESULTS

The performance of the proposed novel safety concept for the introduced impact configurations will be discussed in the following sections. The dynamic accident behaviour and the registered biomechanical loads on the main body parts of the MADYMO dummy were analysed for the primary accident phase, the immediate period after the first contact between the occupant vehicles, here set to 0.3 s after first contact. The kinematics of the motorcycle and rider are shown in detail for five of the seven impact configurations. A quantitative overview of a comprehensive set of injury criteria relative to the respective biomechanical limits (see Table I) for all configurations is given in Fig. 14. Injury risk curves for the most critical body regions, if available, are given. Exemplarily for configuration ⑦, the considered loads and the derivation of the respective injury criteria are provided in Appendix B. The two configurations not shown are (i) ⑤ which is redundant to ④, and (ii) ⑥ with no significant loading in the primary accident phase.

A comparison to a conventional motorcycle without additional safety equipment has not been carried out. Simulations of the proposed motorcycle without its safety equipment would not be an adequate benchmark for improvements in passive safety either. The proposed body has not been designed to prevent or minimize injuries without the equipment as a conventional motorcycle shape would. For conventional motorcycles it is considered advantageous that the rider separates from the motorcycle as soon as possible and does not become entangled in parts of the motorcycle body [7].

Impact Configuration ⑦ (413 – 0/13.4)

According to impact configuration ⑦, the motorcycle impacted at 48 km/h at a right angle into the side of the stationary car right at its centreline. The frontal shape of the motorcycle with its voluminous cockpit fairing and overhanging nose allowed for some deformation structure such as a crash box in front of the stiff fork head with a high contact point. This high contact point prevented the motorcycle from rotating around its transverse/pitch axis after impact, a typical trajectory for motorcycles with no structure in front of the fork head and therefore a load transfer primarily over the lower front wheel.

As shown in Fig. 6, the safety components aim to guide and control the trajectory of the rider. Restrained by the belts, the rider's forward displacement continuously decelerated resulting in a rotating upper body motion. This motion and its kinetic energy were absorbed by the front airbag that supports the head and the upper most part of the chest with a rebound of the torso completely averted. Fig. 7 illustrates that the temporal advance of the belt activation leads to an early restraint of the pelvis. The belt load limiter allows for a continuous, and relative to the motorcycle body, prolonged velocity reduction with lower deceleration.

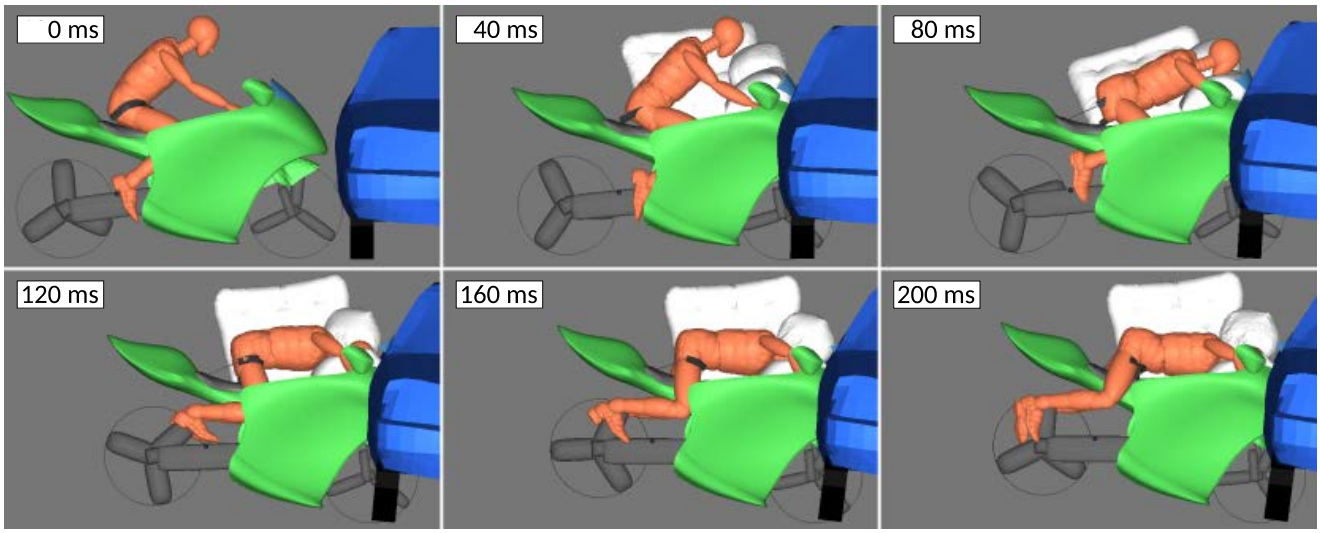

Fig. 6. Accident behaviour for impact configuration ⑦ in the primary impact phase.

The highest observed body loads were safety concept related, i.e. the head, thorax and pelvis accelerations and neck tensile forces. These loads were mainly dependent on the implemented belt load limit, which was selected based on a trade-off between tolerable body loads and minimal forward body displacement. More forward displacement enhances the risk of the rider's head hitting the car and the elongated belts reducing the potential to restrain the rider in the secondary impact phase. As shown in Fig. 8, the highest head acceleration loads (and hence neck tensile forces) were due to the belt restraint up to 100 ms with comparatively smaller loads during airbag impact.

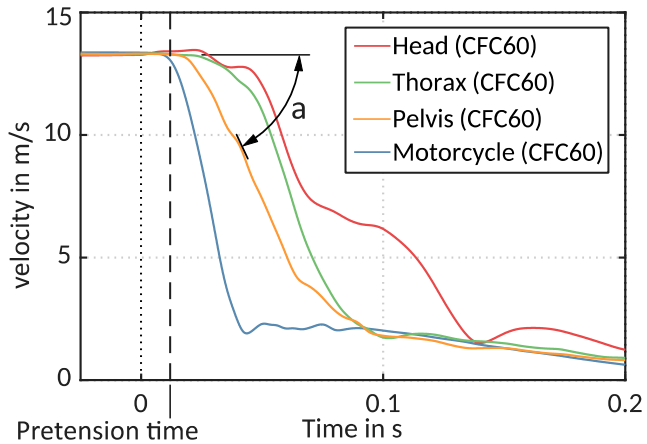

Fig. 7. Motorcycle and motorcyclist's body regions velocity and acceleration for configuration ⑦. The gradient of the curves corresponds to the respective mean acceleration a.

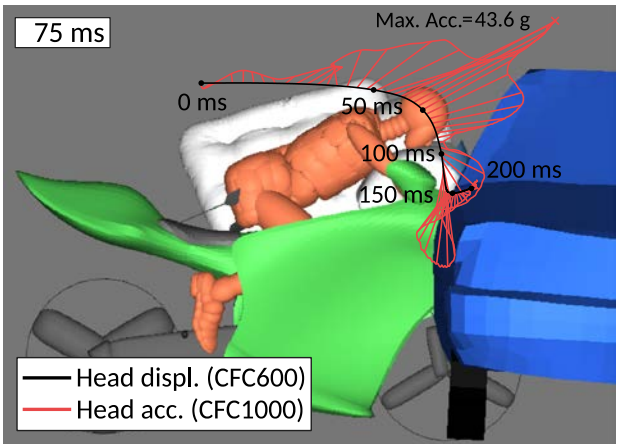

Fig. 8. Head displacement trajectory with resultant linear acceleration relative to reference space for configuration ⑦ of the primary impact phase.

Impact Configuration ③ (413 – 6.7/13.4)

In impact scenario ③ the motorcycle impacted at 48 km/h at a right angle into the side of the car travelling at 24 km/h at its centreline. The intended protective principle of the motorcycle's safety concept is very similar to ⑦. As shown in Fig. 9, the rider's forward displacement continuously decelerated resulting in a rotating upper body motion, here decelerated by the smaller mirror airbag, preventing the head from hitting the car.

Again, the highest simulated body loads were the head, thorax and pelvis accelerations and neck tensile forces as well as neck shear forces. The recorded very high axial femoral forces were compression forces on the left leg when impacting the motorcycle body. As stated before, the intended leg protectors of the passive safety concept have not been included at this stage, with their necessity clearly shown.

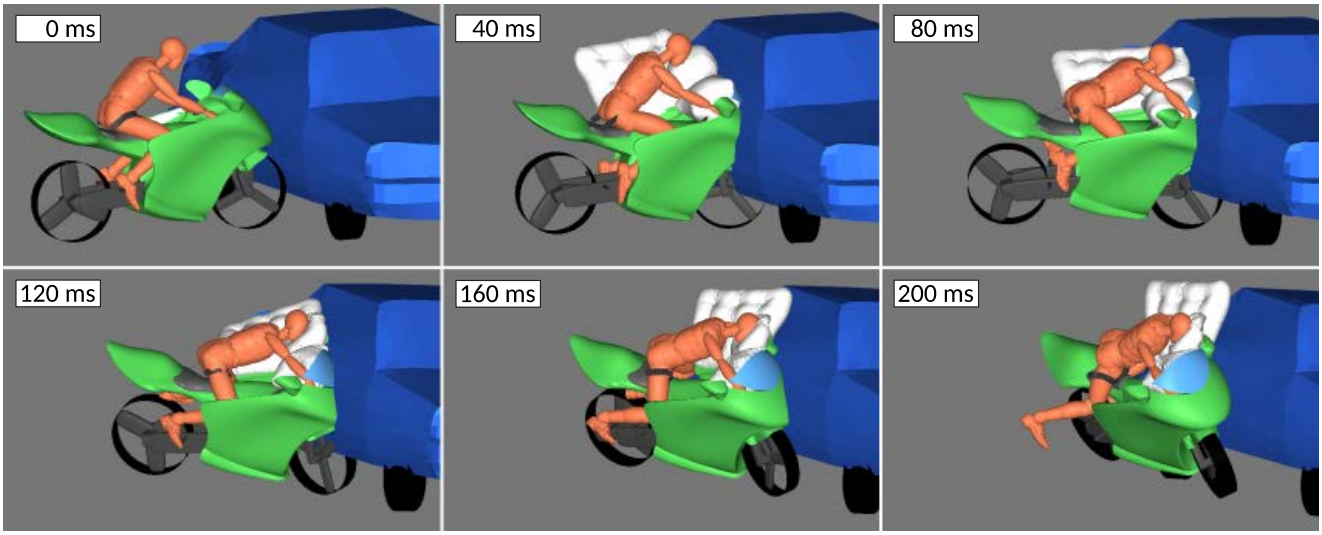

Fig. 9. Accident behaviour for configuration ③ in the primary impact phase.

Impact Configuration ④ (412 – 6.7/13.4)

In impact configuration ④ the motorcycle hit the car that is travelling at 24 km/h at its centre line at a speed of 48 km/h and a relative angle of 45°. The side airbag quickly deployed in between the rapidly diminishing space between the rider and opposing vehicle and prevented the rider from directly impacting into the car (Fig. 10). Here, the side airbag used the lateral face of the car as a reaction structure. For these types of scenarios, where the relative angle between the opposing vehicles is comparatively small, the impact forces are likewise small, and the motorcycle retains a main portion of the initial impact speed. This extends the overall length of the accident with the motorcycle eventually falling over to one side. Therefore, the side airbag is not only intended to protect the rider during the first vehicle impact but also in the following presumably long secondary accident phase. This motivates the airbag design without exhaust holes to keep it inflated for the complete course of a potentially long accident.

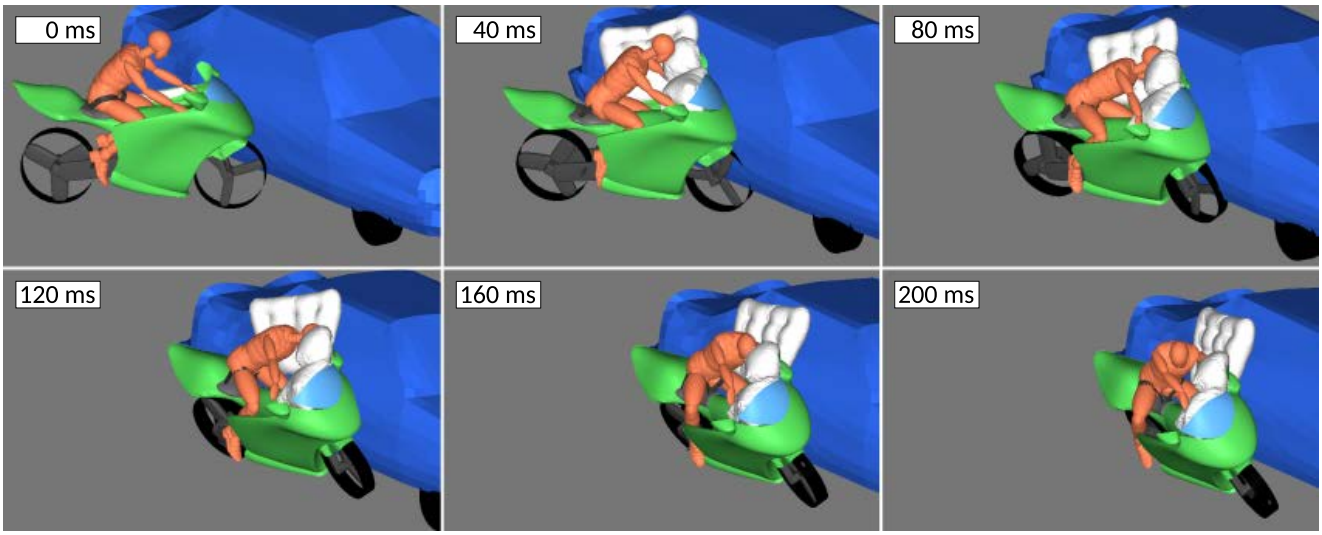

Fig. 10. Accident behaviour for configuration ④ in the primary impact phase.

Here, the highest body loads resulted from impacting into the relatively hard side airbag, since it had no exhaust hole that would lead to a softer absorption of the impact. The substantial loads acted on the head, pelvis and neck, again with high demand of leg impact protection to reduce compression forces of the leg to the motorcycle body impact impulse.

Configuration ⑤ (414 – 6.7/13.4), the same impact configuration at a relative angle of 135°, had a comparable trajectory to ④ with similar crash dynamics and dummy load spectrum for the proposed safety concept. The behaviour of the motorcycle for configuration ⑥ was equivalent in so far that because of the shallow impact angle the primary impact and the simulated dummy loads were negligible with the potential relocation of the accident consequences into a later accident phase.

Impact Configuration ① (143 – 9.8/0)

In impact configuration ① the stationary motorcycle was hit laterally by the car that was travelling at 35 km/h at a relative angle of 90°. The side airbag quickly deployed to the side of the rider, was pushed down by the rider's lateral rotational motion and landed on the car's hard bonnet protecting the rider by cushioning the impact, as shown in Fig. 11. Even more so as for ④ and ⑤, the belts supported the pelvis and ensured that the rider did not slide over the airbag and in the process risking direct head to car contact. The proposed innovative motorcycle body encloses the rider's lower extremities and aims to protect them specifically in these situations.

The simulated body loads were high for the head accelerations and neck tensile forces with the highest loads during airbag impact as illustrated in Fig. 12. In the current MB approach, the undeformed rigid car geometry pierced through the motorcycle geometry, resulting in high femur forces for lateral collision like configurations ① to ⑤.

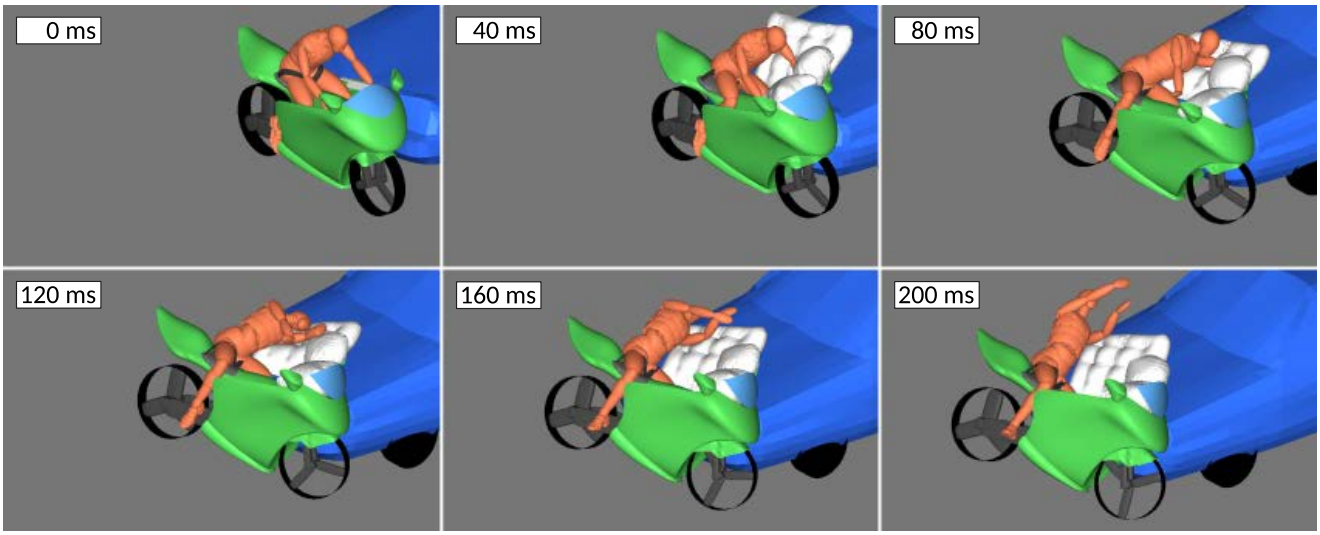

Fig. 11. Accident behaviour for configuration ① in the primary impact phase.

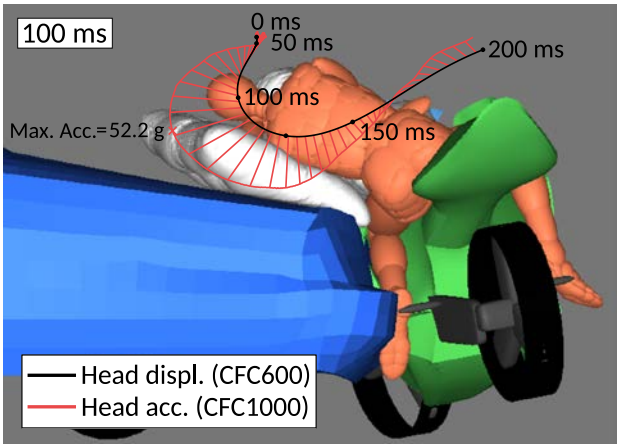

Fig. 12. Head displacement trajectory with resultant linear acceleration relative to reference space for configuration ① for the primary impact phase.

Impact Configuration ② (114 – 6.7/13.4)

Similar to configuration ① the motorcycle was hit by the frontal section of the car. Here the motorcycle travelled at 24 km/h, the car at 48 km/h and the relative angle is 135°. Equivalent to ① the side airbag quickly deployed in between rider and car and absorbed the rotational motion of the rider's upper body using the bonnet of the car as a reaction structure, see Fig. 13. The belts established a pivot point for the guided upper body trajectory and limited the reach of the head within the extent of the airbag. Just like in ① because of the low lateral impact, the motorcycle began to roll around its longitudinal axis. In ② with combined yaw around the vertical axis, this resulted in a multiaxial trajectory of the motorcycle with a partial counter-rotational motion of the rider. The multiaxial trajectory and the potentially long secondary accident phase –the shallow impact angle resulted in a high retained motorcycle velocity – will cause significant challenges to guide the motion of the driver in the secondary accident phase. Here, this resulted in a comparably high neck load spectrum and high pelvis resultant acceleration as illustrated in Fig. 14.

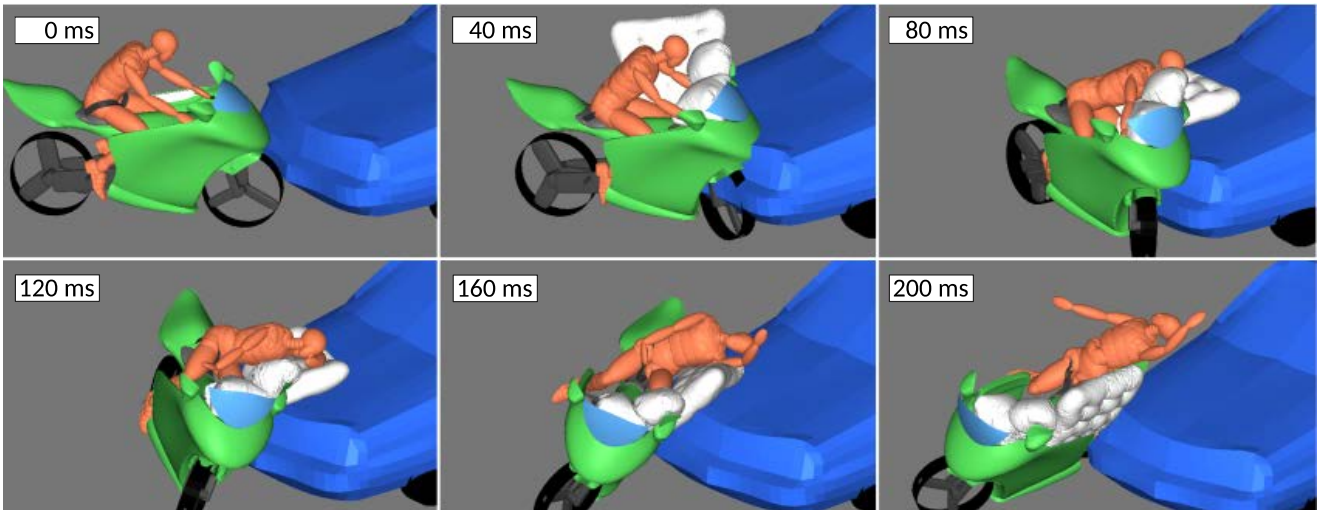

Fig. 13. Accident behaviour for configuration ② in the primary impact phase.

Injury Criteria relative to Biomechanical Limits and Injury Risk Assessment

A correlation between simulated body loads and potential human rider injuries has been made with the set of injury criteria and respective biomechanical limits. In [7] summarised data for relevant body regions of motorised two-wheelers were used. Additionally, to those, the normalized neck injury criterion (NIJ) [12] has been considered, all shown in Table I. Based on these values, Fig. 14 gives an overview of the derived injury criteria normalised to their respective biomechanical limits with a colour code indicating the severity of the body loads.

TABLE I

EVALUATED INJURY CRITERIA WITH RESPECTIVE BIOMECHANICAL LIMITS [7][12]

Body region	Criterion	Abbreviation	Limit
Head	Head Injury Criterion (36 ms)	HIC(36)	1000 for
	Resultant head acceleration	a_{3ms}	80 g over 3 ms
Neck	Neck tensile force	$F_{z,\,tens,\,1ms}$	3.3 kN over 1 ms
		$F_{z,\,tens,\,45ms}$	1.1 kN over 45 ms
	Neck compression force	$F_{z,\,compr,\,1ms}$	4 kN over 1 ms
		$F_{z,\,compr,\,45ms}$	1.1 kN over 45 ms
	Neck shear forces	$F_{xy,\,1ms}$	3.1 kN over 45 ms
		$F_{xy,\,45ms}$	1.1 kN over 45 ms
	Neck rearward moment	$M_{y,\,fwd,\,max}$	57 Nm
	Neck forward moment	$M_{y,\,rwd,\,max}$	190 Nm
	Neck injury criterion	NIJ_{max}	1
Thorax	Resultant thorax acceleration	a_{3ms}	60 g over 3 ms
	Chest deflection	$Defl_{max}$	75 mm
	Viscous Criterion	VC_{max}	1 m/s
Pelvis	Resultant pelvis acceleration	a_{3ms}	60 g over 3 ms
Femur	Femur axial force	$\lvert F_z \rvert_{max}$	10 kN

Generally, the biomechanical limits of the chosen set of injury criteria were met for the primary impact phase except for femoral axial loading caused by dummy to motorcycle contact, not restraint loading. High femoral forces indicate the necessity of leg impact protection located at the motorcycle body, as stated before, currently not considered in this combined MB and FE simulation model phase. Overall, the loading on the body regions was mostly low, since for all the examined accidents a direct impact of the dummy to the opposing vehicle was successfully avoided. Instead, the use of belt restraints and airbags resulted in a steady kinetic energy absorption over a longer time span. The highest loads were due to head, thorax and pelvis accelerations as well as neck tensile forces, mainly dependent on the implemented belt load limit, a trade-off between tolerable resulting body loads and feasible body displacements within reach of the airbags.

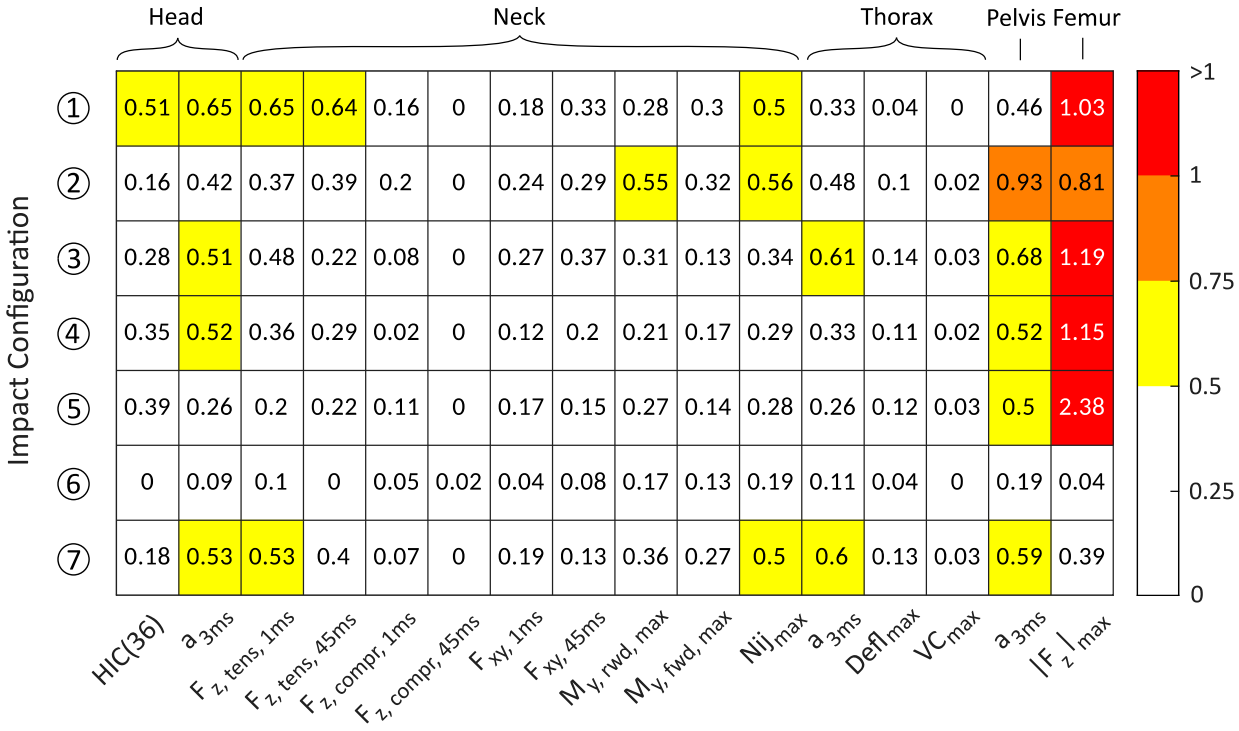

Fig. 14. Injury criteria relative to respective biomechanical limit (from Table I). Values for the primary impact phase, the immediate period after the first contact between the occupant vehicles, here set to 0.3 s.

For significant loads, a classification of the potential injury severity with the abbreviated injury scale (AIS) would be meaningful. Here, injury risk curves for the head injury criterion (HIC) and NIJ were available. Based on injury risk curves for HIC(36) [13] AIS level probabilities are shown in Fig. 15. Risks of AIS3+ for all configurations are not higher than 13.1 % and for all but configuration ① below 8 %. According to injury risk curves for NIJ [12] the risks for AIS3+ are for all the configurations below 11.6 % (Fig. 16).

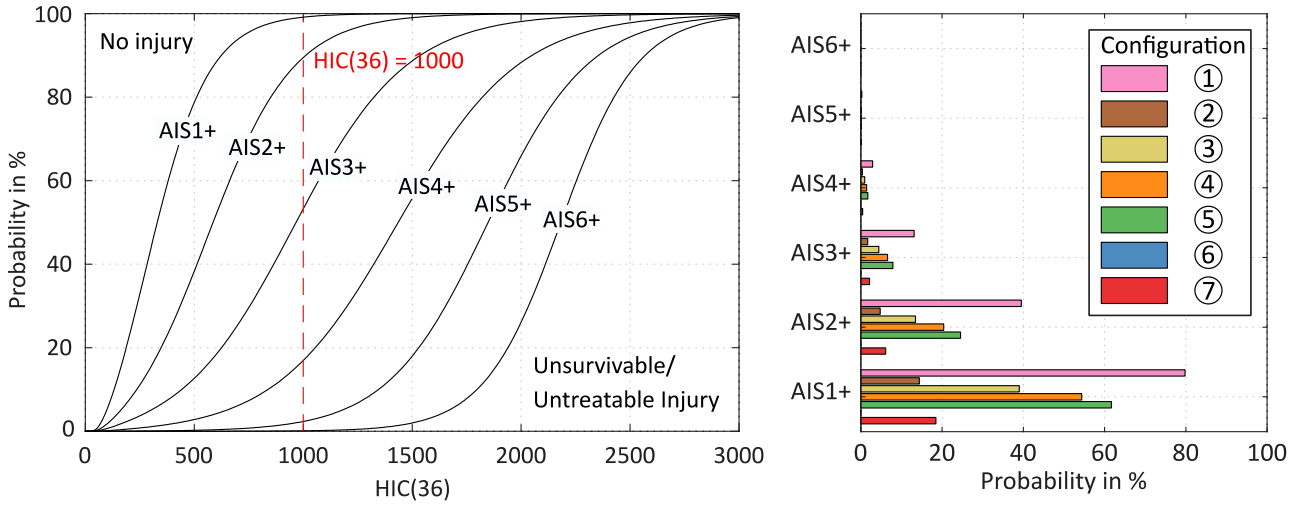

Fig. 15. HIC injury risk curves [13] and AIS level evaluation for configuration ① to ⑦.

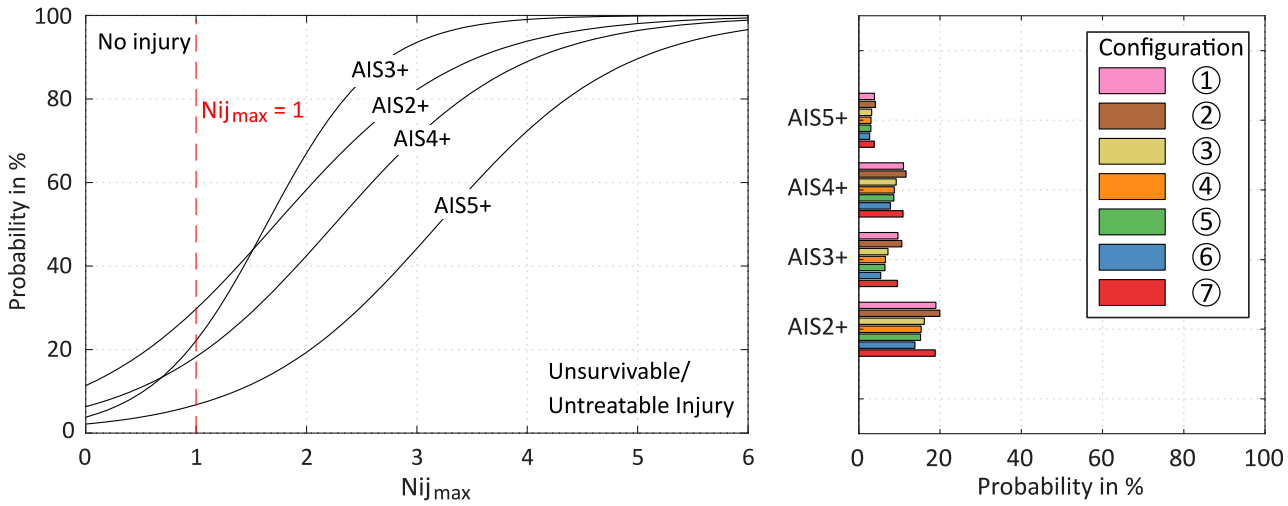

Fig. 16. NIC risk curves [12] and AIS level evaluation for configuration ① to ⑦.

IV. Discussion

Restraining the rider with belts and decelerating the resulting upper body motion relative to the motorcycle with multiple surrounding airbags leads to a guided and controlled dummy trajectory for the primary accident phase. The combination of multiple passive safety systems, the novelty of this safety concept, crucially minimises the intrinsic incalculability of a motorcycle rider's motion in an accident situation. To achieve the controlled trajectory, good compromises had to be found between the component timing and parameters for airbag inflation and belt loading. Here, the advantage of the MB representation with only selective application of FE-components, efficiency with low computational costs, has shown to be essential. It allowed for many design iterations to achieve good performance in very different load cases.

Reference [14] states that current crashworthiness analysis of powered two-wheelers with both MB and FE simulations are not equally systematic to the car field and therefore often have limited qualitative rather than quantitative value. Although in this work the validation capabilities are limited because of the early concept phase and the multitude of assessed impact configurations, some concept specific circumstances are very beneficial. In studies of conventional motorcycle accidents, severe dummy to accident opponent contacts are mostly imminent, with the accurate prediction of contacts between two stiff contact partners like head/helmet and car body often difficult. Here, it is possible to neglect the helmet with its inner and outer contact definition. Also, direct dummy head and upper torso to car contact is avoided, which further eliminates major sources of uncertainty. Except for dummy to motorcycle body contact, all other dummy contacts were reduced to merely MB to FE contacts with compliant FE contact partners, which are far more predictable and validated with crash experiments of passenger cars, for instance [15]. Contact interactions of a dummy with belt restraints and airbags, driven by more established automotive vehicle safety studies, have a higher degree of reliability and predictability. Here, the concept can benefit from the already very advanced airbag and seatbelt systems in automotive engineering as well as the associated advanced virtual development tools.

Because of the wide spectrum of possible varieties of car sizes and shapes and therefore impact behaviour, a comprehensive depiction of the impact behaviour of the proposed motorcycle concept and cars is difficult. This is most likely to affect the reliability and predictability in cases involving configuration ① and ②. Here, the impact occurs at very vehicle-specific individually shaped body parts such as the bumper section and the low contact point leads to the multiaxial motion of the motorcycle. This, in turn, leads to further challenges to predict the trajectory of motorcycle and rider in the secondary accident phase and to advance and develop protective measures to ensure the rider stays in the protected area for the course of the whole accident.

The chosen MB-representation uses approximations and simplifications, potentially influencing the resulting model predictions, as a trade-off for numerical efficiency. This also includes many parameters which contain uncertainty. To further improve the interaction prediction capabilities with less approximations, and to further verify central aspects, such as avoiding pitching of the motorcycle, a more detailed FE approach in the LS-DYNA software environment will follow. This will also include a viscous elastic material model for the necessary leg protection surfaces, further improving the simulation accuracy and protection effectiveness of the safety concept.

V. CONCLUSIONS

The presented simulations and their results indicate promising performance of the safety concept for all the recommended ISO 13232 accident configurations in the primary accident phase. They illustrate an innovative passive safety idea for motorcycles in very different load cases. Comparable to the safety of occupants of automobiles, a combination of several passive safety systems proved to be effective. The resulting loads on the rider are mostly low and generally at least within the researched limits, except for the addressed currently included modelled leg protection. This is done without compromising a motorcycle's specific advantages i.e. as a compact means of transport and without losing its unique driving behaviour.

Besides further improving collision interaction predictability with less uncertainty, facilitating FE-capabilities in the LS-DYNA software environment, future challenges include consideration of a more diverse group of riders and the design and assessment of protective measures in the secondary accident phase such as potential detrimental effects of the rider being belted to the motorcycle. This is especially crucial since the rider is intended to be non-helmeted and without further safety clothing, a potential game-changer, significantly increasing the suitability of motorcycles as commuter vehicles and/or shared mobility solution.

VI. ACKNOWLEDGEMENT

This work is funded by the State Ministry of Baden-Württemberg for Economic Affairs, Labour and Housing Construction within the programme of Innovative Mobility Solutions.

VII. REFERENCES

[1] ACEM "ACEM statistical release 2019", https://www.acem.eu/images/publiq/2019/ACEM-statistical-release-\--2018-figures.pdf. [2020-26-04]

[2] World Health Organization (2018) *Global status report on road safety 2018*, Geneva, Switzerland.

[3] Statistisches Bundesamt (2018) Verkehr: Verkehrsunfälle. Verkehr, **8**(7), 2018.

[4] Grassi, A., Barbani, D., Baldanzini, N., Barbieri, R., Pierini, M. (2018) Belted Safety Jacket: a new concept in Powered Two-Wheeler passive safety, Procedia Structural Integrity*,* **8**: p.573–593.

[5] Murri R. (2007) Sicherheitsgurt für Motorräder - Lösungsansätze, Schutzpotenzial und Crashergebnisse. Verkehrsunfall und Fahrzeugtechnik, **45**(12): p.341–344.

[6] Osendorfer, H., Rauscher, S. (2001) The development of a new class of two-wheeler vehicles. *Proceedings of the 17th Intern. Technical Conference on the Enhanced Safety of Vehicle,* 2001, Amsterdam, The Netherlands.

[7] Berg, F.A., *et al.* (2011) Bundesanstalt für Straßenwesen*, Prüfverfahren für die passive Sicherheit motorisierter Zweiräder*, Bergisch Gladbach, Germany.

[8] ISO 13232:2005. (2005) Motorcycles – Test and analysis procedures for research evaluation of rider crash protective devices fitted to motorcycles.

[9] Engel, A. (1992) Bundesanstalt für Straßenwesen, *Airbag für motorisierte Zweiräder*, Bergisch Gladbach, Germany.

[10] Hiemer, M. (2005) *Model based detection and reconstruction of road traffic accidents*, p.207. Universitätsverlag Karlsruhe, Karlsruhe, Germany.

[11] Kuroe, T., Namiki, H., Iijima, S. (2005) Exploratory study of an airbag concept for a large touring motorcycle: Further research second report. *19th International Technical Conference on the Enhanced Safety of Vehicles,* 2005, Washington DC, United States.

[12] Eppinger, R., *et al.* (1999) National Highway Traffic Safety Administration, *Development of Improved Injury Criteria for the Assessment of Advanced Automotive Restraint Systems – II,* Washington DC, United States.

[13] National Highway Traffic Safety Administration "Injury Risk Curves and Protection Reference Values", https://one.nhtsa.gov/cars/rules/rulings/80g/80GII.html. [2020-29-03]

[14] Barbani, D., Pierini, M., Baldanzini, N. (2014) Development and validation of an FE model for motorcycle–car crash test simulations. International Journal of Crashworthiness, **19**(3): p.244–263.

[15] National Highway Traffic Safety Administration "Crash Simulation Vehicle Models", https://www.nhtsa.gov/crash-simulation-vehicle-models. [2020-29-03]

VIII. APPENDIX

Appendix A: Simulations of full-scale crash tests SH 01.01 and SH 99.32 performed by Dekra

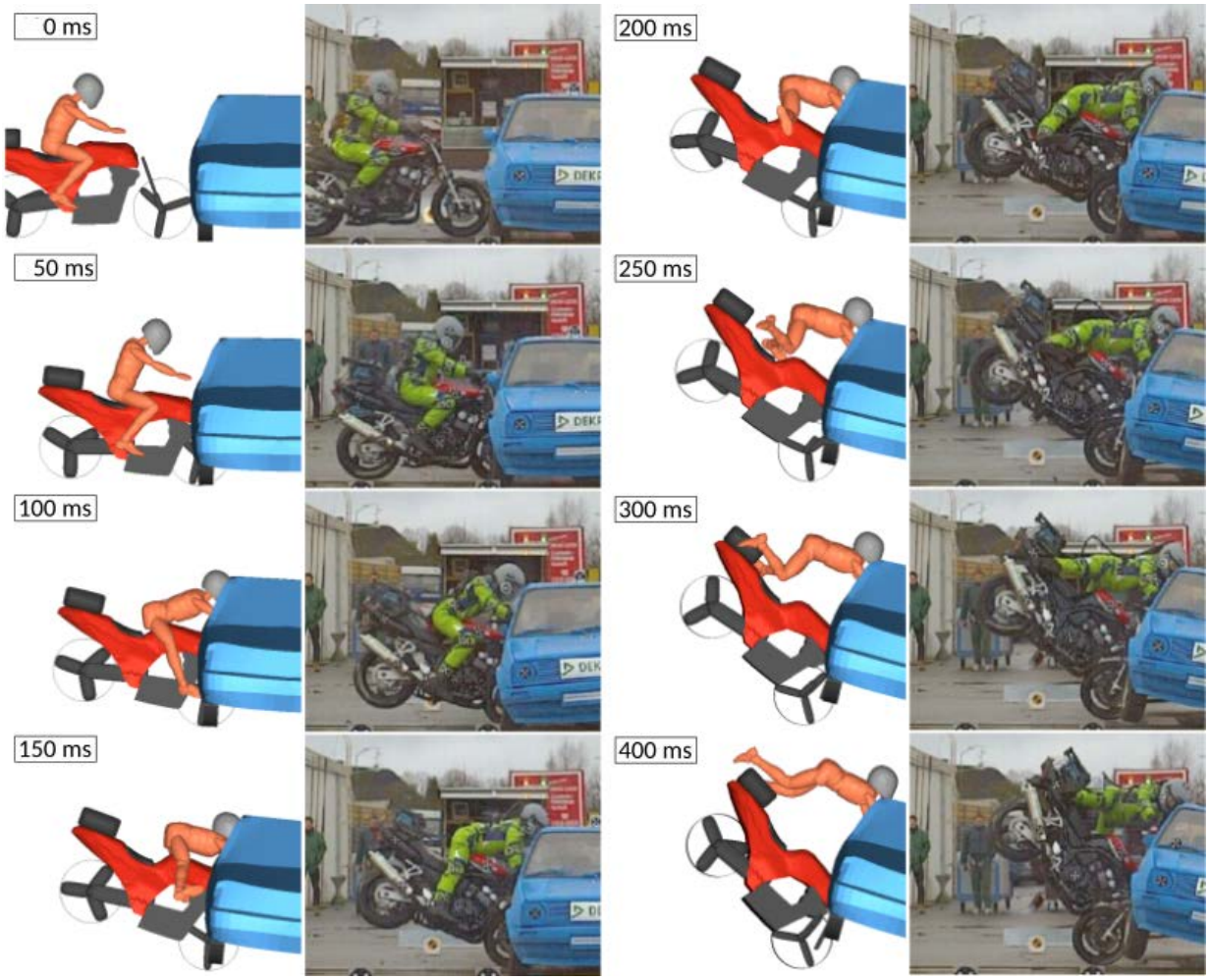

Fig. A1. Simulation of Dekra crash test SH 01.01 [7]; ISO 13232 configuration ⑦ (413 – 0/13.4) of Yamaha FZS 600 Fazer and helmeted Hybrid III 50th percentile in sitting configuration against VW Golf II.

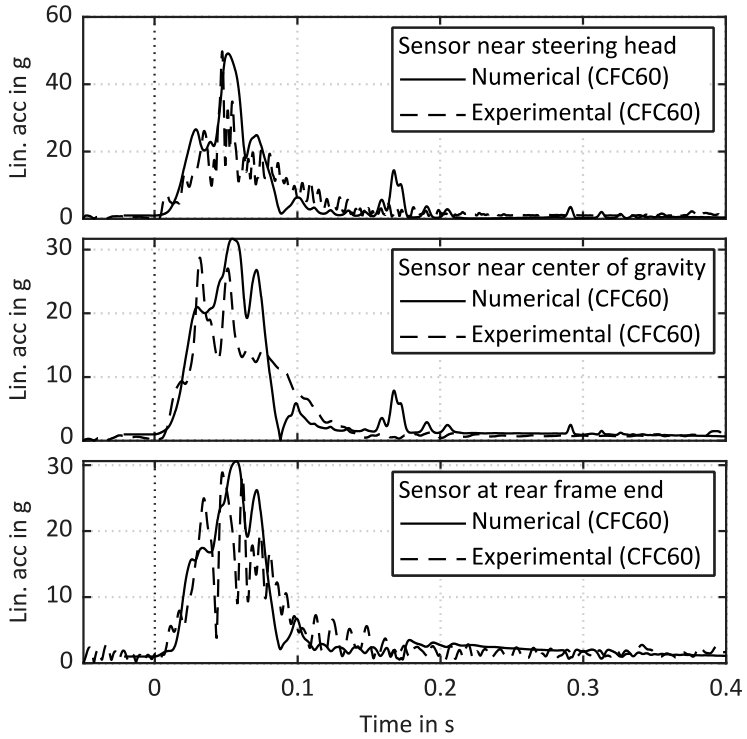

Fig. A2. Acceleration sensor data of Yamaha FZS 600 Fazer according to Dekra test documentation for SH 01.01.

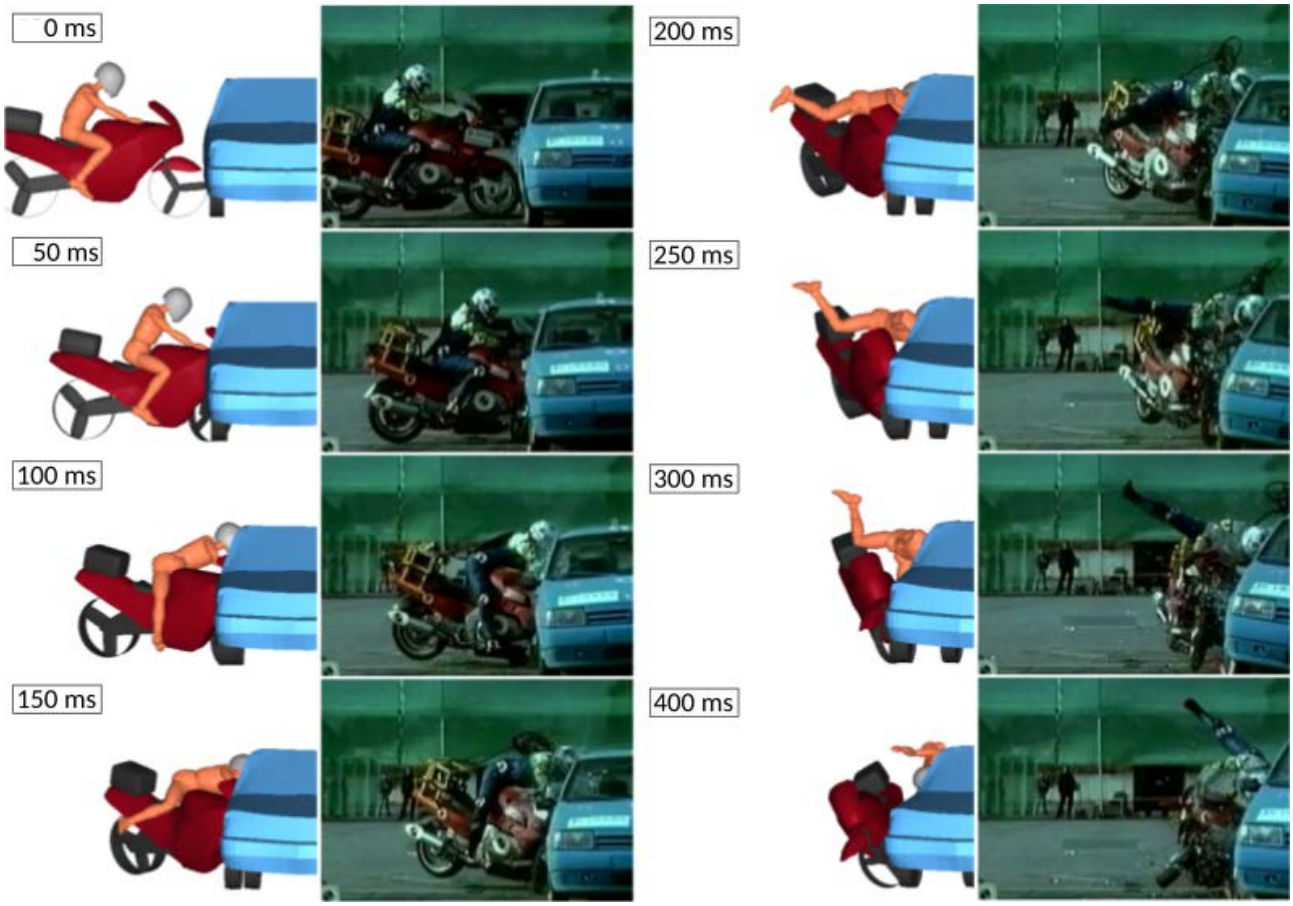

Fig. A3. Simulation of Dekra crash test SH 99.27 [7]; ISO 13232 configuration ③ (413 – 6.7/13.4) of Yamaha GTS 1000 and helmeted Hybrid III 50th percentile in sitting configuration against Fiat Tipo 1400.

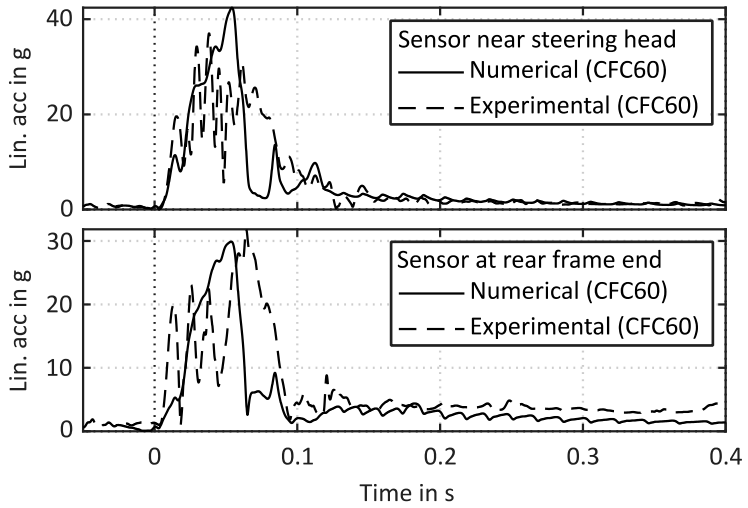

Fig. A4. Acceleration sensor data of Yamaha GTS 1000 according to Dekra test documentation for test SH 99.27.

Appendix B: Dummy loads and determined injury criteria for impact configuration ⑦ (414 – 6.7/13.4)

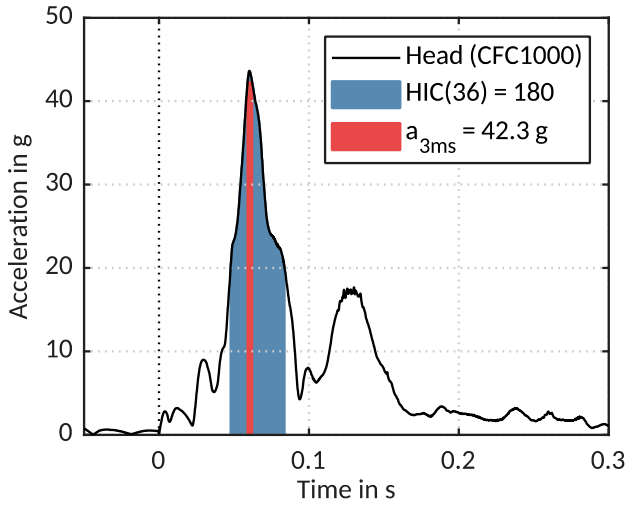

Fig. B1. Head linear acceleration for configuration ⑦.

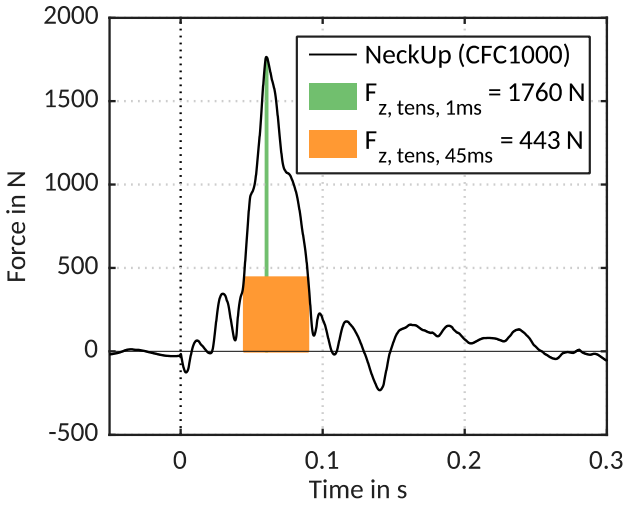

Fig. B2. Neck tensile force for configuration ⑦.

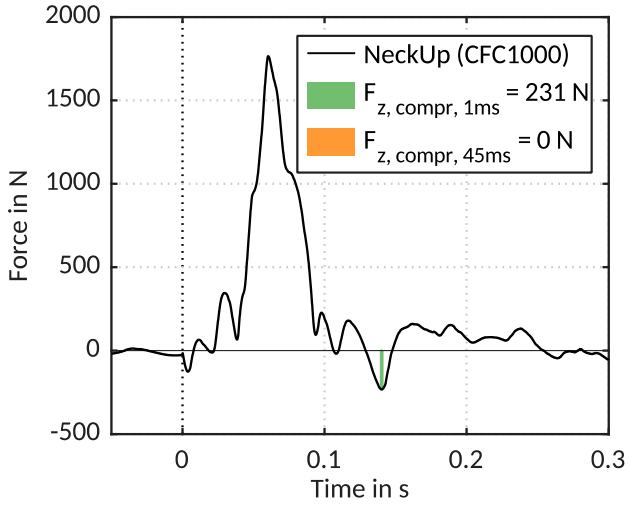

Fig. B3. Neck compression force for configuration ⑦.

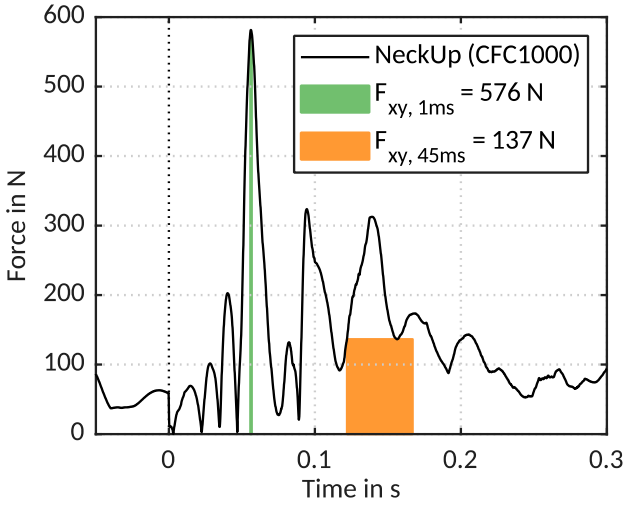

Fig. B4. Neck shear forces for configuration ⑦.

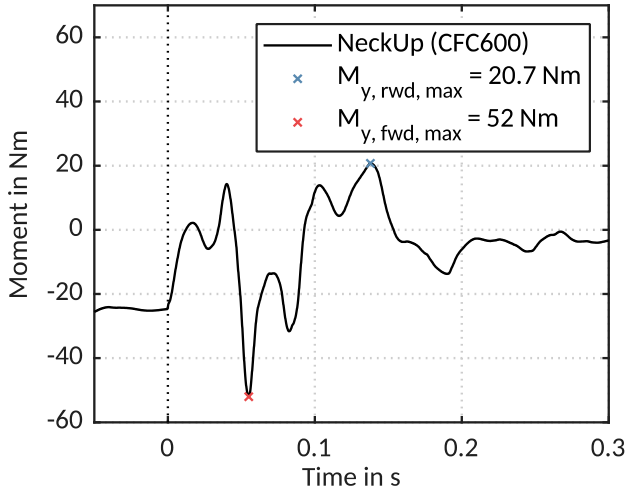

Fig. B5. Neck flexion and extension moment for configuration ⑦.

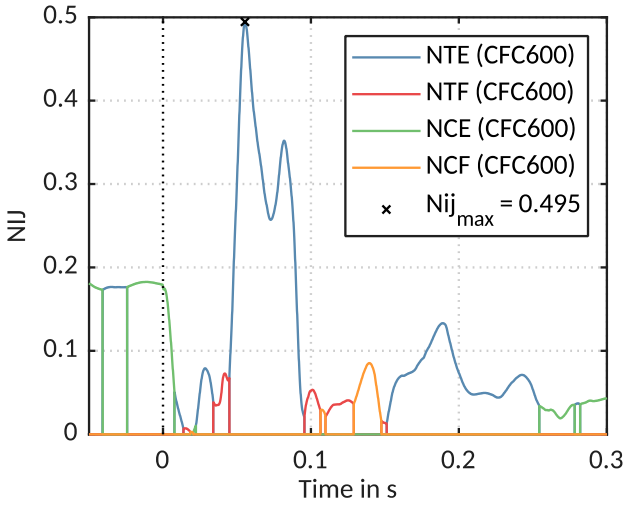

Fig. B6. Neck injury criterion for configuration ⑦.

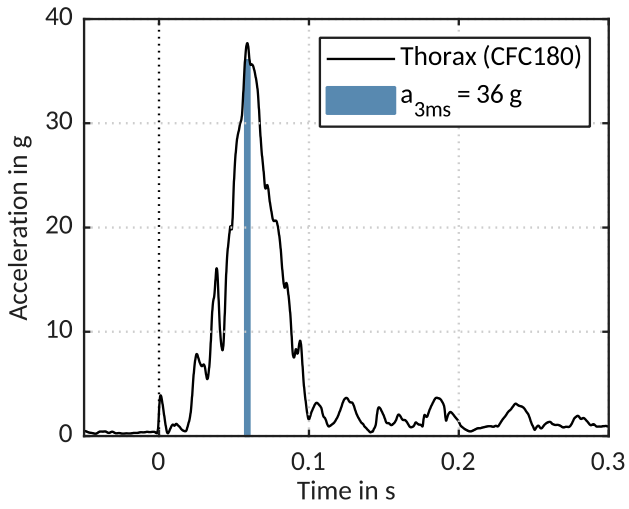

Fig. B7. Thorax linear acceleration for configuration ⑦.

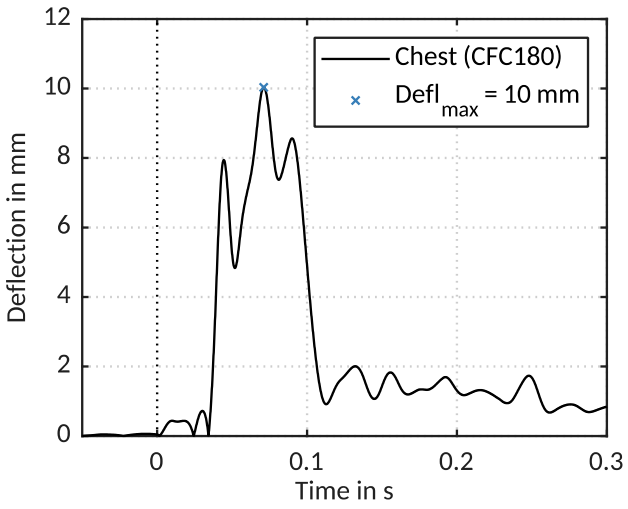

Fig. B8. Chest deflection for configuration ⑦.

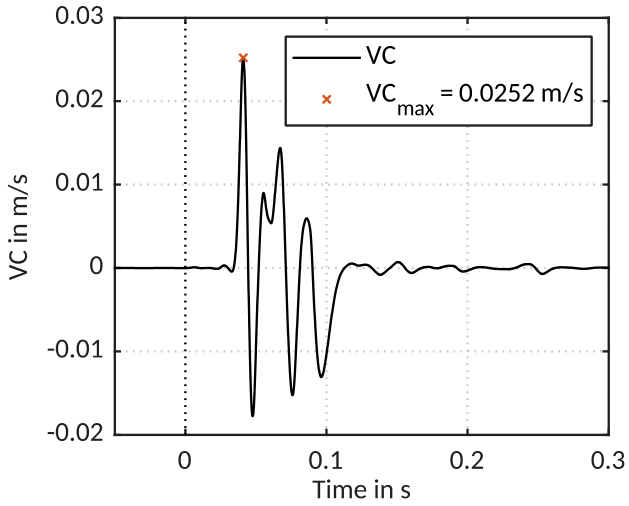

Fig. B9. Thorax viscous criterium for configuration ⑦.

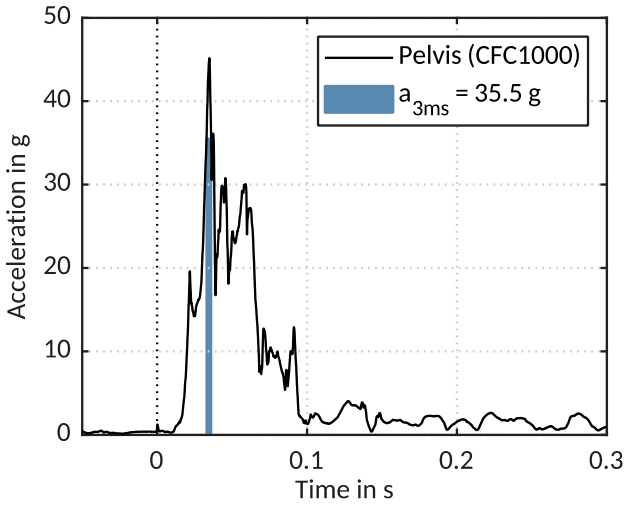

Fig. B10. Pelvis linear acceleration for configuration ⑦.

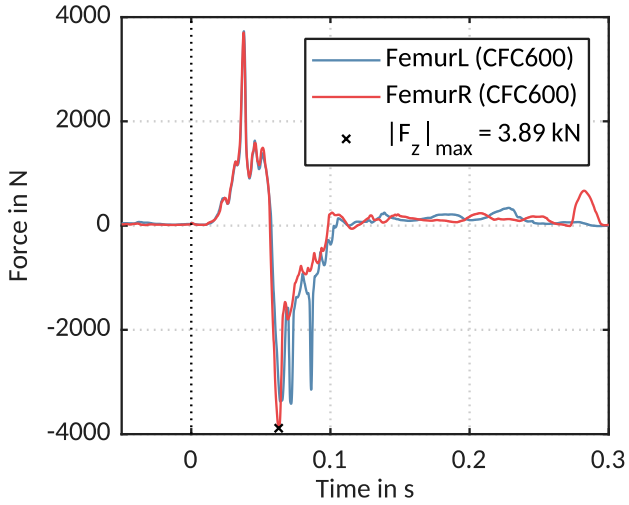

Fig. B11. Femur axial forces for configuration ⑦.